ysis (North-Holland, Amsterdam, 1968).
[10]G. A. Bartholomew *et al.*, Nucl. Data A3, 367 (1967).
[11]R. Hardell and C. Beer, Physica Scripta 1, 85 (1970).
[12]C. E. Moss, Nucl. Phys. A170, 111 (1971).
[13]E. K. Warburton, J. W. Olness, and A. R. Poletti, Phys. Rev. 160, 938 (1967).
[14]See for instance: P. Hvelplund and B. Fastrup, Phys. Rev. 165, 408 (1967); J. H. Ormrod, Can. J. Phys. 46, 497 (1968); and references contained in these works.
[15]D. Powers and W. Whaling, Phys. Rev. 126, 61 (1962); J. A. Davies, F. Brown, and M. McCargo, Can. J. Phys. 41, 829 (1963); M. McCargo, J. A. Davies, and F. Brown, Can. J. Phys. 41, 1231 (1963); T. Anderson and G. Sorenson, Can. J. Phys. 46, 483 (1968); and B. Domeij, F. Brown, J. A. Davies, and M. McCargo, Can. J. Phys. 42, 1624 (1964).
[16]D. H. Wilkinson, in *Nuclear Spectroscopy*, edited by F. Ajzenberg-Selove (Academic, New York, 1960), Pt. B, p. 862 ff.
[17]B. H. Wildenthal, E. C. Halbert, J. B. McGrory, and T. T. S. Kuo, Phys. Rev. C 4, 1266 (1971).
[18]F. C. Erné, Nucl. Phys. 84, 91 (1966).
[19]B. Rosner and E. J. Schneid, Phys. Rev. 139, B66 (1965).
[20]P. Hvelplund, Kgl. Danske Videnskab. Selskab, Mat.-Fys. Medd. 38, No. 4 (1971).
[21]J. M. G. Caraça, R. D. Gill, P. B. Johnson, and H. J. Rose, Nucl. Phys. A176, 273 (1971); E. Wong, B. C. Robertson, K. V. K. Iyengar, D. M. Sheppard, and W. C. Olsen, Nucl. Phys. (to be published).

PHYSICAL REVIEW C VOLUME 6, NUMBER 1 JULY 1972

Nuclear Lifetimes of States in Na^{22}, Ne^{22}, and P^{30} by the Recoil-Distance Method*

Franklin D. Snyder†
Department of Physics and Astronomy, The University of Iowa, Iowa City, Iowa 52240
(Received 9 August 1971)

The recoil-distance method was used to measure electromagnetic transition probabilities in Na^{22}, Ne^{22}, and P^{30}. Na^{22} and Ne^{22} were produced from the 6.4-MeV He^4-on-F^{19} reaction. P^{30} was produced from the 6.4-MeV He^4-on-Al^{27} reaction. The mean lives in psec were: $Ne^{22}_{1.275\to0}$, 5.9± 1.1; $Na^{22}_{0.891\to0}$, 16.1± 3.0; $Na^{22}_{1.528\to0}$, 4.5± 0.8; $P^{30}_{0.709\to0}$, 53± 10.

I. INTRODUCTION

Electromagnetic transition probabilities (lifetimes) provide valuable information about the character of a nuclear excited state. The lifetime, along with the spin, parity, and other spectroscopic values, is used to compare and contrast various nuclear models. Electromagnetic transitions are particularly useful because they provide unambiguous nuclear information from the well-understood electrodynamic-transition-probability matrix elements. Most lifetimes that are longer than 10^{-15} sec are measured by the delayed-coincidence technique, the recoil-distance method (RDM), or Doppler-shift attenuation method (DSAM).

The RDM is a valuable tool to measure lifetimes in the 10^{-12}- to 10^{-10}-sec region. This technique is useful in bridging the gap between the delayed-coincidence method and the DSAM. The plunger variant of the RDM, which was used in this investigation, was first used by Severiens and Hanna[1] in 1956. Jones *et al.*[2] and others[3,4] have described the RDM in great detail.

A RDM measurement reveals the lifetime of a nuclear state by correlating the time for decay of a reaction by-product nucleus to its kinematic flight time. Figure 1 illustrates the ideal RDM experiment. A beam of high-energy (6.40-MeV) particles passes through a thin foil which supports the target material on the down-beam side. Excited nuclei, which are produced in the target by nuclear reactions, leave the target with a velocity which is predictable from the kinematics of the reaction. As an excited nucleus leaves the target with a velocity v, it has a probability of decaying in flight and therefore emitting a Doppler-shifted $E_f = E_0(1 + v/c)$ γ ray in the laboratory system. If the nucleus has not decayed after it has traveled a distance D, then it is quickly (~10^{-13} sec) stopped by a high-Z stopping material (stopper). When the stopped nucleus finally decays, it will decay with the normal energy E_0 (neglecting the γ recoil). A high-resolution Ge(Li) γ detector is used to detect both the stopped and Doppler-shifted photons.

The probability of a γ ray being emitted from a nucleus in flight is

$$p_f = \frac{1}{t}\int_0^t e^{-t/\tau}\,dt = \frac{1}{D}\int_0^D e^{-x/v\tau}\,dx = \frac{v\tau}{D}(1 - e^{D/v\tau}) , \tag{1}$$

where v is the flight speed, D the stopper distance, τ the mean life of the state being studied, and $x = vt$. The probability of a γ ray being emitted from

a stopped nucleus is

$$p_0 = \frac{1}{D}\int_D^\infty e^{-x/v\tau}\,dx = \frac{v\tau}{D}e^{-D/v\tau}. \quad (2)$$

If

$$R = \frac{p_0}{p_0 + p_f} = e^{-D/v\tau}, \quad (3)$$

then

$$\tau = -D/v\ln R. \quad (4)$$

τ is linear in D in this parametrization.

A discussion of the RDM method has been given previously[2] in which a graphical approximation procedure is suggested for cases where the experimental γ-ray resolution is insufficient to resolve the stopped and flight components. The present report describes (Sec. III) a method whereby the experimental data for such cases can be handled by a least-squares-fitting procedure, in which the flight component is described, at any arbitrary distance D, in terms of the flight distribution observed experimentally for $D=\infty$. This procedure extracts lifetime information from both the predictable shape of the Doppler component and the ratio of stopped to total γ-ray intensity. This method should be used for those cases where the kinematics are such that the two components cannot be experimentally resolved.

The states investigated were chosen to be populated by low-Q-value reactions. A low-Q value gives the kinematic advantage of confining the recoiling nuclei to a direction close to the beam axis, which lessens the broadening of the Doppler-shifted flight peak. The following reactions were used to investigate the indicated lifetimes:

(1) $F^{19}(He^4, n)Na^{22}$ 0.891, 1.528 MeV $Q = -1.9505$;

(2) $F^{19}(He^4, p)Ne^{22}$ 1.275 MeV $Q = 1.6747$;

(3) $Al^{27}(He^4, n)P^{30}$ 0.709 MeV $Q = -2.6458$.

The He^4-on-F^{19} experiment was performed to check out the apparatus and to confirm the lifetimes that have not been so thoroughly investigated. The $Al^{27}(He^4, n)P^{30}$ experiment was performed to check the lifetime of the 0.709 – 0.0-MeV transition, which has shown disagreement between a DSAM[5] measurement and a RDM[6] measurement. Since the RDM is generally a better technique than the DSAM for lifetimes greater than a few psec, this experiment was expected to give better results. Figure 2 illustrates the energy levels[7,8] of the states investigated.

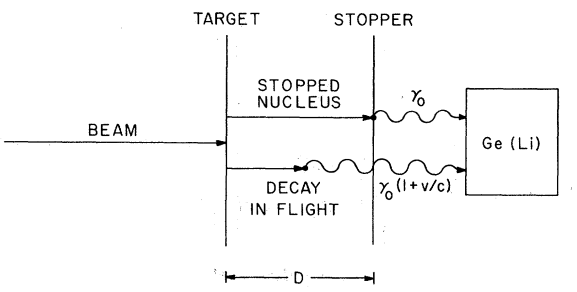

FIG. 1. Schematic diagram of the plunger technique.

II. EXPERIMENTAL DESCRIPTION

The 6.4-MeV He^4 beam was provided by The University of Iowa's model CN Van de Graaff accelerator. The beam is analyzed and regulated by a 90° magnet to ±0.3%.

The target and stopper are contained in a high-conductance vacuum chamber fitted with a liquid N_2 cold ring for optimum vacuum conditions. The beam enters the rear of the chamber through a pair of collimators, with final beam collimation done on a block 2 in. from the target. The beam spot is 3 mm in diameter.

Typical speeds for recoiling nuclei are of the order of mil/psec (mil = 0.001 in.). To measure lifetimes in the psec range, it is necessary to know and maintain the separation and planarity of the target and stopper to accuracies of the order of 0.1 mil.

The target foil and stopper were mounted on nearly identical blocks using Jones's[2] technique of stretching the foil over a rubber ring to remove wrinkles. The stopper was a foil similar to the target foil which could be replaced when contaminated or damaged. Both the stopper and target backing were 1-in.-diam 0.05-mil-thick copper foils. Copper was used rather than nickel because

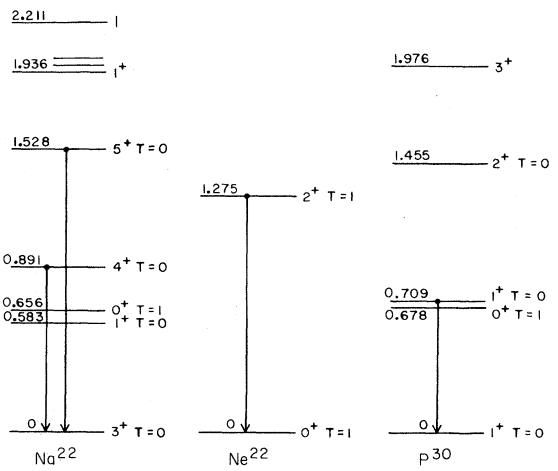

FIG. 2. Energy-level diagrams of the nuclei investigated. Energies are in MeV.

of its higher heat conductivity (Cu = 0.90, Ni = 0.14 cal/ sec cm^{-1} $°K^{-1}$). From the geometry of the chamber, it was calculated that a 250-nA 6.4-MeV He^4 beam spot on a nickel foil would have a 280°C temperature rise at the center, but that a copper foil would only have a 45°C temperature rise.

Calculations that compare the thermal expansion from beam heating to the amount of prestretching the foil can have, constrained by the elastic limit, indicate that the foil might loosen in an extreme situation. If the foil did loosen, the resulting bow could make the target-stopper distance strongly dependent on the beam current. This effect was investigated by measuring the ratio of stopped to total peak for the 0.891 state of Na^{22} induced by a 6.4-MeV He^4 beam on a 60-μg CaF_2 target supported by a 0.05-mil nickel foil. The stopper for this test was a solid block of copper. For beam currents of 250 and 40 nA no change in the ratio was observed.

It is concluded that the strain of the foil is sufficient to compensate for thermal expansion induced by beam heating. Alexander[9] has reached the same conclusion looking for a change in capacitance between the target and stopper with the beam on and off.

The stopper foil was thick enough to stop the heavy recoiling nuclei, but thin enough to let the incident beam pass through to be stopped 3.5 in. later on a piece of tantalum. The tantalum was mounted on an insulated Faraday cup which contained the cold ring.

The facing surfaces of the target block and the stopper block were ground and polished to an overall planarity of better than 0.1 mil. The surface that supports the foil was planar to better than 0.02 mil. The stopper and target were held a distance D apart from one another by an arbor shim spacer.[10] The whole assembly is held together with three screws which are equally torqued into place.

Distortions caused by squeezing the blocks together were investigated with a double-exposure hologram.[11] A conventional hologram picture was taken of the blocks squeezed together with two screws torqued to 60 in. lbs and with the third screw torqued to only 10 in. lbs. The third screw was then torqued to 60 in. lbs without disturbing the blocks and the hologram was reexposed. The resulting hologram showed dark bands wherever the two exposures differed in separation by a half-integral number of wavelengths of light (~0.01 mil). The area which supports the foil had only one fringe across it, which indicates a distortion of the order of only 0.01 mil even in this extreme differential-stress situation.

Solid spacers provide an excellent way to insure planarity between the target and stopper. The thinnest shim used was 1 mil. These shims have an over-all thickness tolerance of ±0.2 mil and a uniformity of better than 0.01 mil per in. The relative spacings were determined to ±0.05 mil by measuring the differential separation of the blocks with a comparer before and after the shim stocks were inserted.

The $F^{19}(He^4, n)Na^{22}$ and $F^{19}(He^4, p)Ne^{22}$ experiments were performed on a 60-$\mu g/cm^2$ CaF_2 target, prepared by simple evaporation from a tantalum boat at high vacuum. The $Al^{27}(He^4, n)P^{30}$ experiment was performed on a 60-$\mu g/cm^2$ Al target evaporated from a tungsten wire basket.

The γ rays were detected with a 25-cm^3 trapozoidal Ge(Li) detector that was 10 cm from the target. The detector was surrounded with 2-in.-thick paraffin-boron blocks to slow down and absorb neutrons that might cause lattice defects in the Ge(Li) detector, and thereby impare its resolution. The system resolution for the 709-keV line was 3.3 keV.

The laboratory data were processed in three stages.[12] First, a background of the form $Y = ae^{bX}$ was subtracted by fitting to the wings of the peak. The resulting spectra were fitted to a linear combination of a stopped- and flight-peak response function obtained at $D = 0$ and $D = \infty$, respectively. Finally, these ratios were fitted to a decaying exponential plus background.

III. ANALYSIS OF DATA

Since some of the emitting nuclei can have velocities off the z axis (incoming beam direction), the γ flight peak will have some broadening. This broadening will be a function of the angular distribution of the excited nuclei [$\sigma(\theta)$], the kinematic

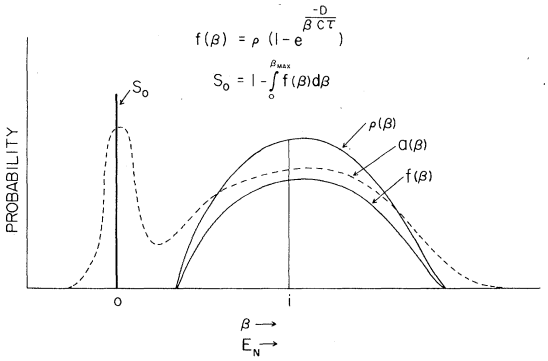

FIG. 3. Schematic diagram of peak shape, ignoring detector and solid-angle broadening. S_0 is the stopped peak, f the flight peak at an arbitrary distance, and ρ the flight-peak shape at $D = \infty$. The dashed line indicates the experimental shape when broadening is included.

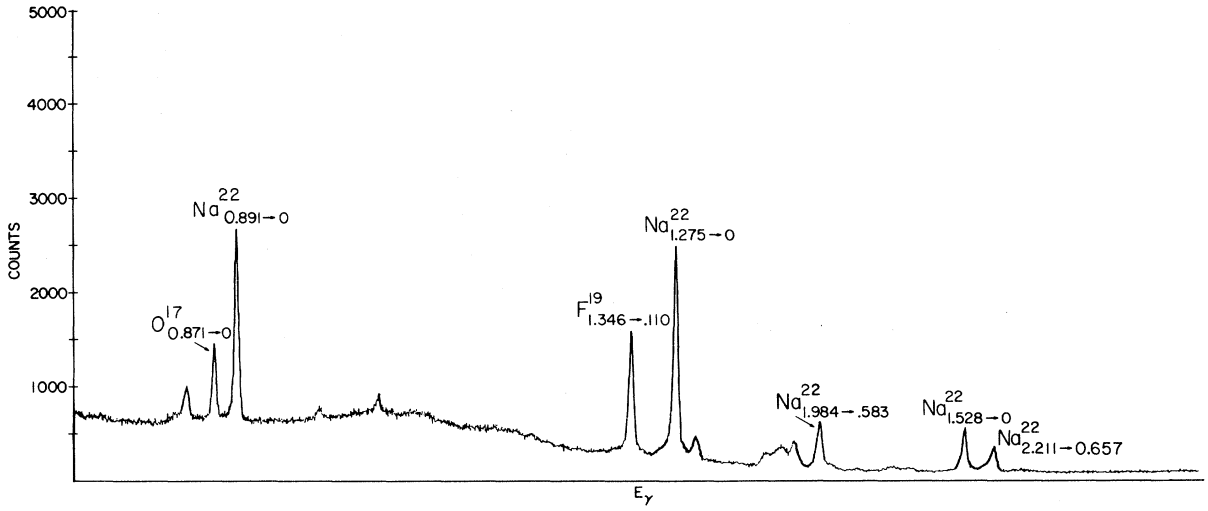

FIG. 4. Full γ spectra from $F^{19}(He^4,n)Na^{22}$ and $F^{19}(He^4,p)Ne^{22}$ experiments at $D=0$ mil.

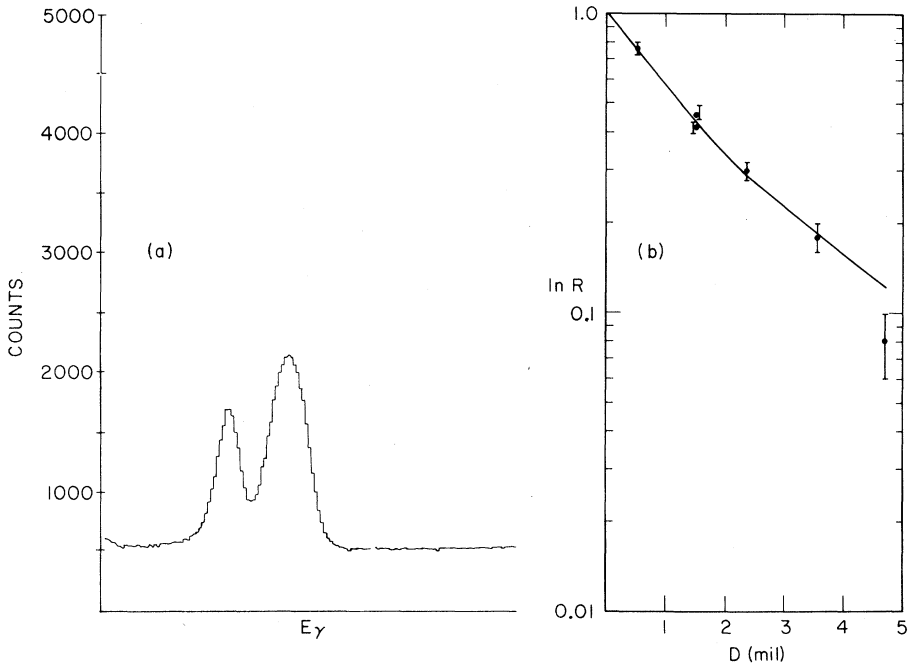

FIG. 5. (a) Expanded spectra of the 0.891→0-MeV transition of Na^{22} from the reaction $F^{19}(He^4,n)Na^{22}$ at $D=2.35$ mil. (b) Graph of R vs D for the 0.891→0-MeV transition of Na^{22} from the reaction $F^{19}(He^4,n)Na^{22}$.

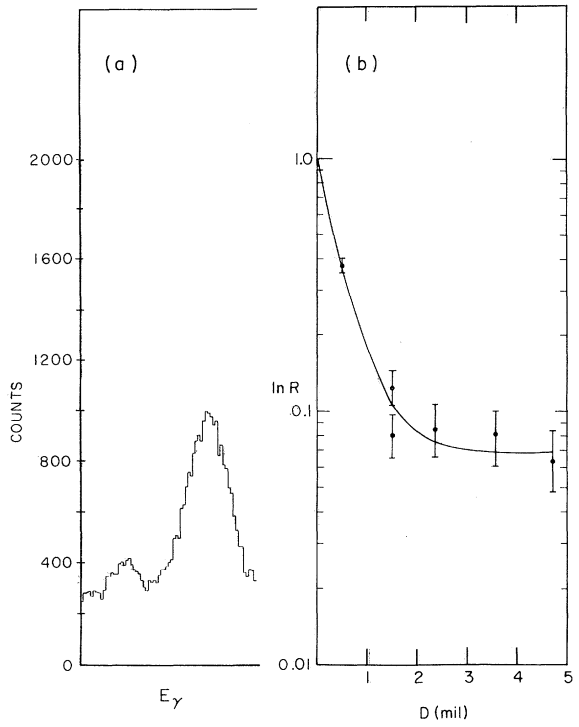

FIG. 6. (a) Expanded spectra of the 1.528→0-MeV transition of Na^{22} from the reaction $F^{19}(He^4, n)Na^{22}$ at $D = 1.50$ mil. (b) Graph of R vs D for the 1.528→0-MeV transition of Na^{22} from the reaction $F^{19}(He^4, n)Na^{22}$.

velocity $[v(\theta)]$, the particle-γ angular correlation, the finite angular diameter of the γ detector, and the detector-electronic broadening. Figure 3 illustrates the shape of the γ spectra if isotropy is assumed for the particle-γ angular correlation, and the broadening due to finite detector size and resolution are ignored. The horizontal axis can be taken as either the Doppler-shifted γ energy or as $\beta(\theta) = [v(\theta)/c]\cos\theta$, since a cardinal correspondence exists between these quantities for the reactions considered. β is the component of the relative speed of the nuclei along the z axis. S_0 is the stopped peak, $f(\beta)$ the flight-peak shape, and $\rho(\beta)$ the flight-peak shape at $D = \infty$. With the normalization

$$\int_0^{\beta\ \max} \rho(\beta)d\beta = \int_0^{\beta\ \max} f(\beta)d\beta + S_0 = 1\,, \tag{5}$$

$\rho(\beta)$ becomes the probability that a nucleus will be created with perpendicular speed β. If a nucleus has a perpendicular speed β, then the probability that it will survive to be stopped a perpendicular distance D away is given by

$$p_0(\beta) = e^{-D/\beta C\tau}\,. \tag{6}$$

The decay probability is

$$p_f(\beta) = 1 - e^{-D/\beta C\tau}\,. \tag{7}$$

The flight-peak shape then is given by[3] the product

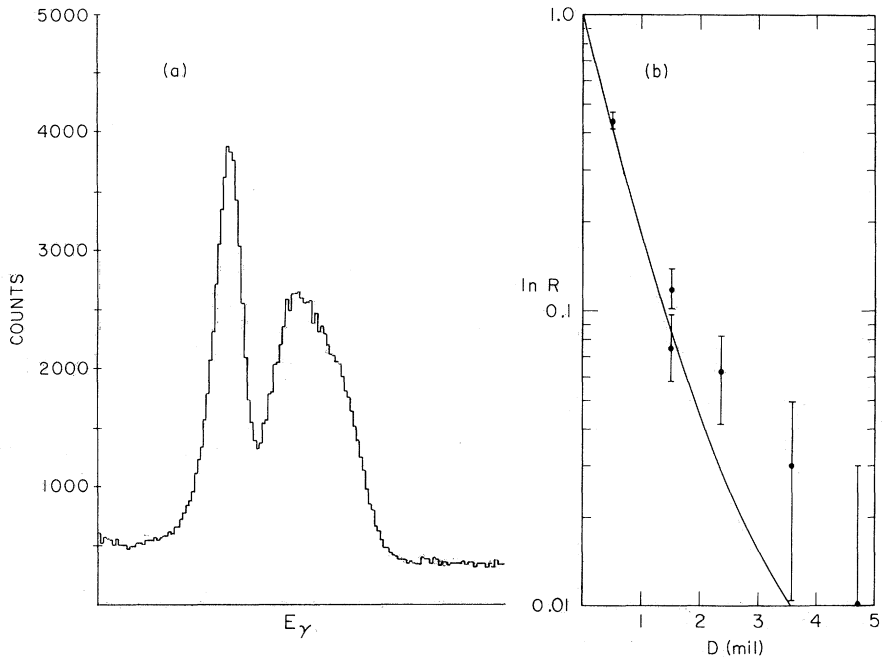

FIG. 7. (a) Expanded spectra of the 1.275→0-MeV transition of Ne^{22} from the reaction $F^{19}(He^4, p)Ne^{22}$ at $D = 0.50$ mil. (b) Graph of R vs D for the 1.275→0-MeV transition of Ne^{22} from the reaction $F^{19}(He^4, p)Ne^{22}$.

of the probability that a nucleus will be created with a perpendicular speed β and the probability that this nucleus will decay in flight:

$$f(\beta)=\rho(\beta)(1-e^{-D/\beta C\tau}). \tag{8}$$

Equation (8) was used to adjust the shape of the flight-peak response function if the flight peak was broadened due to off-axis recoils.

The velocity distribution $\rho(\beta)$ for the recoiling nuclei was determined from the shape of the stopped peak and flight peak at $D=\infty$. If $P(\beta)$ is the observed broadened flight peak at $D=\infty$, and $g(\beta)$ the observed broadened stopped peak representing the broadening function, then the unbroadened flight-peak shape $\rho(\beta)$ at $D=\infty$ can be found from the kernel of the following Fredholm equation of the first kind,[13]

$$P(\beta)=\int_{-\infty}^{+\infty}\rho(\beta-B)g(B)\,dB. \tag{9}$$

It was assumed that g was a Gaussian with half-width h_0, and P an asymmetric Gaussian with half-widths h_l and h_r. Unconvoluting Eq. (9) yields ρ to also be an asymmetric Gaussian with half-widths $\eta_l=(h_l^2-h_0^2)^{1/2}$ and $\eta_r=(h_r^2-h_0^2)^{1/2}$. h_0, h_l, and h_r were found by least-squares fitting to the Gaussians described above.

The absolute distances D_j were determined from the relative distances by fitting well-known lifetimes with τ fixed and the D_j's free to change their absolute values collectively. That is $D_j(\text{absolute})=D_j(\text{relative})+d_0$ for all j. The d_0 obtained in this way was consistent for all the lifetimes fitted.

R_j was determined for each distance D_j and the resulting R_j vs D_j values were nonlinear least-squares-fitted to the following form after R was corrected[2] for solid angle and efficiency effects,

$$R(\text{corrected})_j=\frac{\sum_{i=1}^{N}\rho_i(\beta_i)e^{-D_j/\beta_i C\tau}+H}{1+H}. \tag{10}$$

ρ_i is the flight-peak probability in channel i with $\beta=\beta_i$ described above. τ and H are the only free parameters in the fit.

IV. RESULTS

Figure 4 shows the full spectra obtained in the He^4-on-F^{19} experiment. The laboratory peaks and decay curves for these states are illustrated in Figs. 5–7. The small constant background for these states suggests that the background-stopped peak was primarily caused by F^{19} contamination rather than γ cascades from isomeric states. Since the Na^{22} states were populated near threshold, the flight peaks from these states were well resolved from the stopped peaks. The flight peak from the Ne^{22} state was kinematically broadened, which introduced error into the "R" fits for this state. However, as can be seen from Fig. 5(a), the flight peak for the $Ne^{22}_{1.275}$ peak is noticeably narrower on the low-energy side, which made the fit less ambiguous. A contamination was present under the flight peak of the $Ne^{22}_{1.275\to 0}$ transition (see Fig. 4). To correct for its effect, the background-subtraction routine subtracted a fraction of the contaminant peak from the flight peak, adjusting the ratio to the size of the adjacent free background. This contamination was checked to be the same at the beginning and end of the He^4-on-F^{19} experiment.

Figure 8 shows the full spectra obtained in the He^4-on-Al^{27} experiment. The laboratory peak and

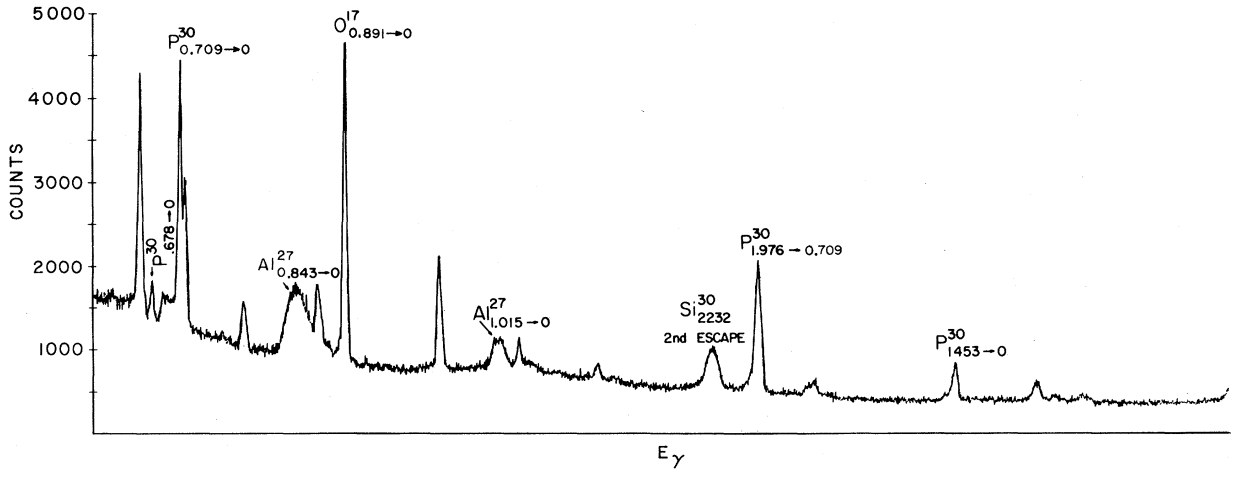

FIG. 8. Full γ spectra from the $Al^{27}(He^4,n)P^{30}$ experiment at $D=2.35$ mil.

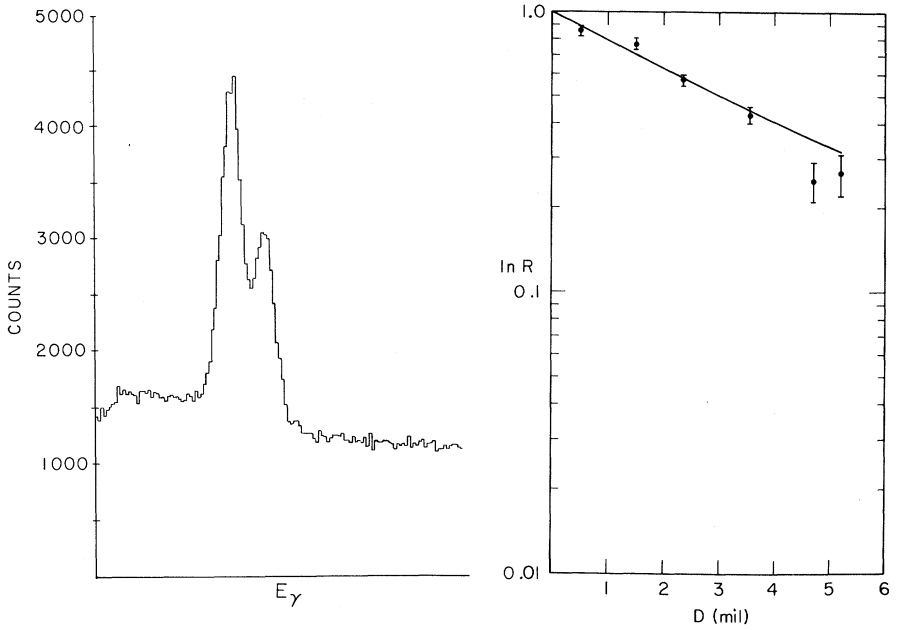

FIG. 9. (a) Expanded spectra of the 0.709→0-MeV transition of P^{30} from the reaction $Al^{27}(He^4,n)P^{30}$ at $D=2.35$ mil. (b) Graph of R vs D for the 0.709→0-MeV transition of P^{30} from the reaction $Al^{27}(He^4,n)P^{30}$.

decay curve for the 0.709→0-MeV transition of P^{30} is shown in Fig. 9. The 0.709→0-MeV transition produced a mean lifetime of $\tau = 53 \pm 10$ psec. This is in good agreement with an earlier RDM[7] value of 55 ± 7 psec and disagrees with the results of a DSAM[6] measurement which indicated $\tau = 22 \pm 5$ psec. The DSAM measurement used the two-stopper method to slow down the decaying nucleus in Al and 5.0 atm of CO_2 gas. DSAM measurements are generally not attempted for lifetimes much greater than ~5 psec, since stopping powers are not well known for the slow velocities that a nucleus has that is so long lived. Shielding effects[2] for nuclei as large as P^{30} can cause significant reduction in the stopping power of a gas, causing an observed lifetime to appear shorter than it actually is. Since stopping-power information is not necessary for the RDM measurement, it is felt that the DSAM value is too short.

The results of this investigation are summarized in Table I. The references for other measurements of these lifetimes are noted in the table. General agreement is noted in all the lifetimes except the 0.709-MeV state of P^{30}. Warburton, Poletti, and Olness[7] and Henson *et al.*[8] have discussed the theoretical interpretations of the states investigated.

TABLE I. Summary of results.

Reaction	Decay (MeV)	Mean life (psec) This work	Mean life (psec) Average of others
$F^{19}(He^4, p)Ne^{22}$	1.275→0	5.9±1.1	4.7±0.5 [a]
$F^{19}(He^4,n)Na^{22}$	0.891→0	16.1±3.0	14.2±0.7 [b]
	1.528→0	4.5±0.8	4.2±0.5 [b]
$Al^{27}(He^4,n)P^{30}$	0.709→0	53.0±10.0	22±5 [c] 55±7 [d]

[a] References 2, 3, and S. J. Skorka, J. Hertel, and T. W. Retz-Schmidt, Nucl. Data A2, 347 (1966).
[b] References 2 and P. Paul, J. W. Olness, and E. K. Warburton, Phys. Rev. 173, 1063 (1968).
[c] Reference 5.
[d] Reference 6.

ACKNOWLEDGMENTS

The author wishes to thank R. T. Carpenter for suggesting this experiment and R. R. Carlson for many helpful discussions.

*Work supported in part by the National Science Foundation.

†Present address: University of Kentucky, Lexington, Kentucky.

[1]J. C. Severiens and S. S. Hanna, Phys. Rev. 104, 1612 (1956).

[2]K. W. Jones, A. Z. Schwarzschild, E. K. Warburton, and D. B. Fossan, Phys. Rev. 178, 1773 (1969).

[3]R. J. Nickles, Nucl. Phys. A134, 308 (1969).

[4]A. Z. Schwarzschild and E. K. Warburton, Ann. Rev. Nucl. Sci. 18, 265 (1968).

[5]R. E. Pixley and A. R. Poletti, Bull. Am. Phys. Soc. 14, 125 (1969).

[6]F. Haas, B. Heusch, G. Frick, A. Gallmann, and D. E. Alburger, Nucl. Phys. A156, 385 (1970).

[7]E. K. Warburton, A. R. Poletti, and J. W. Olness, Phys. Rev. 168, 1232 (1968).

[8]S. H. Henson, S. Cochavi, M. Marmor, and D. B. Fossan, Phys. Rev. C 3, 191 (1971).

[9]T. K. Alexander and A. Bell, Nucl. Instr. Methods 81, 22 (1970).

[10]Precision Stell Warehouse, Inc., Downers Grove, Illinois.

[11]K. S. Pennington, Sci. Am. 218(No.2), 40 (1968).

[12]F. D. Snyder, University of Iowa Research Report No. 71-29 (unpublished).

[13]N. H. Marshall, AEC Report No. IDO-17175 (unpublished).

PHYSICAL REVIEW C VOLUME 6, NUMBER 1 JULY 1972

Angular Distribution of K Electrons Ejected During K Capture by Polarized Nuclei

R. L. Intemann

Department of Physics, Temple University, Philadelphia, Pennsylvania 19122

(Received 22 October 1971)

The angular distribution of the K electrons ejected during allowed K-capture transitions in polarized nuclei is calculated using a formalism previously developed by the author. It is shown that a result having a relative accuracy of order $Z\alpha$ may be obtained through the use of nonrelativistic electronic wave functions and a "semirelativistic" Coulomb Green's function due to Glauber and Martin. The result shows that, contrary to the predictions of previous theories, there is a noticeable asymmetry in the angular distribution of the ejected electrons, the asymmetry parameter being approximately a linear function of the electron's momentum. Possible experimental tests of the theory are described.

I. INTRODUCTION

The continuous spectrum of electrons ejected by atoms undergoing orbital electron capture has been the subject of a number of investigations. These began with the work of Primakoff and Porter[1] in which the intensity of the spectrum of the K electrons ejected during allowed K-capture transitions was calculated using the sudden perturbation approximation. Over the next ten years this theoretical work was followed by reports from several groups[2-6] of observations on the spectra of a number of K-capturing nuclei.

As the experimental data became more refined, certain discrepancies with the Primakoff-Porter theory began to appear[5,6] suggesting a need for more accurate theoretical work. This led the author[7,8] to carry out detailed calculations of the electron spectrum using a more elaborate formalism than that employed by Primakoff and Porter. While these calculations did not succeed in eliminating the reported discrepancies, they did bring refinements to the Primakoff-Porter theory which are especially important for heavy nuclei.[9] In addition, they elucidated the mechanisms responsible for electron ejection and established the relative importance of a number of factors which can affect the process.

All of the above studies dealt with unpolarized nuclei. In this case the ejected electrons are distributed isotropically and the most detailed information on the process is obtained from a study of the ejected-electron energy spectrum.

If, on the other hand, the initial nuclei are polarized, one may carry out angular-distribution studies on the ejected electrons as well. Of experimental interest is the forward-backward asymmetry of the ejected-electron distribution as a function of energy where a comparison with theory does not require a knowledge of the source strength (unlike the case of energy-spectrum measurements). Such directional-distribution studies provide us with a rather different way of testing the basic theory of the K-shell process. Of course, directional-distribution studies are also of value in providing us with information on the properties of nuclear states and as a means of demonstrating the parity-nonconserving property of the weak in-